Liquid Crystals
Publication details, including instructions for authors and subscription information:
http://www.informaworld.com/smpp/title~content=t713926090

The semi-phenomenological model of antiferroelectricity in chiral smectic liquid crystals I. The structure of short pitch modes and a thermodynamical approach

S. Pikin; M. Gorkunov; D. Kilian; W. Haase

Online publication date: 06 August 2010

To cite this Article Pikin, S. , Gorkunov, M. , Kilian, D. and Haase, W.(1999) 'The semi-phenomenological model of antiferroelectricity in chiral smectic liquid crystals I. The structure of short pitch modes and a thermodynamical approach', Liquid Crystals, 26: 8, 1107 — 1114

To link to this Article: DOI: 10.1080/026782999204129

URL: http://dx.doi.org/10.1080/026782999204129

LIQUID CRYSTALS, 1999, VOL. 26, NO. 8, 1107–1114

The semi-phenomenological model of antiferroelectricity in chiral smectic liquid crystals
I. The structure of short pitch modes and a thermodynamical approach

S. PIKIN*, M. GORKUNOV
Institute of Crystallography, Russian Academy of Sciences, Leninskii prosp. 59, 117333 Moscow, Russia

D. KILIAN and W. HAASE
Institut für Physikalische Chemie, Technische Universitat Darmstadt, Petersenstr. 20, 64287 Darmstadt, Germany

(*Received 19 December 1998; accepted 22 February 1999*)

The development of the model of short pitch modes for ferro-, antiferro- and ferri-electric chiral smectic liquid crystals is presented. Prediction of the structures of the subphases is made. The pure short pitch mode having an n-ray star structure of the n-layers of the unit cell appears to possess antiferroelectric properties. Ferrielectricity is assumed to arise as a result of the coexistence and interaction of the short pitch mode with a long pitch helix. Corresponding polarizational properties and fine structure of the peaks of the resonant X-ray scattering from such structures are calculated.

1. Introduction

A number of models have been proposed [1–9] to explain the existence of the many ferro-, ferri- and antiferro-electric phases in chiral liquid crystalline materials. The various Ising models [1–4] take into account relatively large radii of the intermolecular interactions, the interactions being changed in sign dependent upon the distance between molecules. The physical reason for this may be related to long range smectic correlations with an effective correlation length ξ which is larger than the molecular length l. Such effects arise due to steric intermolecular repulsion and to the effects of excluded volume [2]. These models give a qualitative understanding of the role of long range smectic correlations, but they are very limited with respect to possible director orientations. The 'bilayer' model [5–7] proposes a two-layer repeating unit. The proposed 'clock' structure [8] allows for the change in azimuthal director angle between adjacent layers of a constant value. The short pitch modes (SPM) approach [9] describes antiferro- and ferri-electric phases as structures with certain 'families' of modulation modes which have wave numbers close to some rational numbers, the quantities of such 'family members' being limited by the above mentioned smectic correlations.

According to the latter model, inside an area of size ξ along the crystalline axis z, without taking into account the effects of chirality, dipoles are oriented along the polar axis with equal probability for several directions in the smectic planes. This means that the energies of all these states are equal and they determine the main term in energy. Dependent on the packing possibilities for molecules, we can describe these states, i.e. SPM, by the distribution function $\exp(i\pi kz)$ with wave numbers $k = m/nl$ where $m = 1, 2, \ldots, n = \pm m, \pm(m+1), \ldots$. The periods (pitches) of such structures $2nl/m$, where $2n/m$ is an integer, are equal or larger than double the molecular length, but they should be smaller than the radius ξ, i.e. the wave numbers k have a sense if they are larger than 1ξ, i.e. if $n/m < \xi/l$. In such a case, the main term in energy can be presented in the form $\sin^2(m\pi/ql)$; it is equal to zero at $q = k$, but sharply increases at $q \neq k$. Thus, for a fixed m, the SPM with n smaller than $m\xi/2l$ can really exist. If the ratio n/m is larger than ξ/l, then modulations with small q should be taken into account, the main term in the free energy being proportional to q squared. In both the cases (large and small values of the wave number), the main term is independent of the sign of q.

*Author for correspondence.

In the present paper, we develop the SPM model to describe in more detail the structural changes, phase transitions and phase diagrams related to antiferroelectric phenomena.

2. The model assumptions

In general, the order parameter, as a two-dimensional vector Ξ in smectics with inclined molecules, should be presented as the sum

$$\Xi(z) = \sum_j \Xi_j(z) \tag{1a}$$

$$\Xi_{jx}(z_s) = a_j^s \cos(\pi q_j z_s), \quad \Xi_{jy}(z_s) = b_j^s \sin(\pi q_j z_s) \tag{1b}$$

$$\sum_{s=1}^{s=2n/m} a_n^s \cos(\pi k_n z_s) = 0, \qquad \sum_{s=1}^{s=2n/m} b_n^s \sin(\pi k_n z_s) = 0 \tag{1c}$$

$$[a_n^s \cos(\pi k_n z_s)]^2 + [b_n^s \sin(\pi k_n z_s)]^2 = \Theta_n^2(z_s) \tag{1d}$$

where z_s are the coordinates of the smectic layers in the unit cell with size $2nl/m$, $\Theta_j(z_s)$ is the amplitude (tilt angle) of the j-wave (mode) with wave number q_j at the point z_s, the magnitudes a_n^s and b_n^s being equal when the n-wave (mode) is the only one, i.e. it does not go together with other modes. The conditions (1 c) describe the total zero polarization in the unit cell for the n-mode. For the n-SPM, the director projections on the xy-plane at points z_s have absolute magnitudes $\Theta_n(z_s)$, and their orientations form the n-star; the star rays make azimuthal angle $\Psi_s = (s-1)m\pi/n$ relatively to the $s=1$ layer in the ideal antiferroelectric n-star.

The true director being inclined from the crystalline axis z at the angle $\Xi = \Xi(z)$, function $\Xi(z)$ in fact describes a complicated spatial director distribution along the z-axis, the 'weight' of each mode being characterized by amplitudes $\Theta_j(z_s)$ (as the mode structural factor describing its presence in the total structure). For example, a non-zero polarization in the unit cell (the ferrielectric situation) can exist when the antiferroelectric n-mode coexists and interacts with a long-pitch mode (LPM) characterized by wave number q_L. In such a case, the true director is inclined at the same angle Ξ, but, at each point z_s, the director orientation differs from the orientation dictated by the pure antiferroelectric n-mode. This means that the director, lying at the same cone surface with angle Ξ in each smectic layer (i.e. the thickness of smectic layers does not change), exhibits azimuthal deviations at points z_s from the positions determined by the symmetry of the n-mode.

In order to estimate the details of structure of the SPM attenuated by the LPM, it is worth considering the case of small LPM amplitude. While studying the corresponding deformation of a unit cell, the LPM can be considered as a small external displacement, characterized by the two dimensional vector $\mathbf{D}$, which results in the single layer contribution to the uncompensated polarization in the unit cell. Then, the star rays make new azimuthal angles Ψ_s which slightly deviate from their values in the ideal star, and the small corrections $\Delta\Psi_s$ are proportional to the components D_x and D_y:

$$\Delta\Psi_s = c_s^{(1)} D_x + c_s^{(2)} D_y. \tag{2}$$

Due to the symmetry of the unperturbed star, we expect that this correction diminishes for the ray that is initially oriented along vector $\mathbf{D}$. Therefore we can write

$$\Delta\Psi_s = d \sin(\Psi_s - \varphi_D) \tag{3}$$

where φ_D is the azimuthal angle of the $\mathbf{D}$ vector and d is the coefficient to be determined. Correspondingly, the unit cell polarization components in the deformed star are equal to

$$\frac{2n}{m} D_x = -d\Xi \sum_{s=1}^{2n/m} \sin\Psi_s \sin(\Psi_s - \varphi_D) \tag{4a}$$

$$\frac{2n}{m} D_y = d\Xi \sum_{s=1}^{2n/m} \cos\Psi_s \sin(\Psi_s - \varphi_D). \tag{4b}$$

After the summation in equation (4) we obtain $d = -(2D/\Xi)$. Then, by equations (2) and (3), constants $c_s^{(1)}$ and $c_s^{(2)}$ can be found.

For example, we consider the 3-mode unit cell ($m=2$, $k_3 = 2/3l$) with the smectic layer coordinates $z_1 = 0$, $z_2 = l$, and $z_3 = 2l$. In the absence of the long pitch mode, i.e. of a displacement $\mathbf{D}$ with projections D_x and D_y along given axes in the cell, director projections $\Xi_3(z_s)$ on the xy-plane at points z_s form the 3-star with equal rays shown in figure 1 (a). In the presence of a constant displacement $\mathbf{D}$ with projections D_x and D_y, the director exhibits azimuthal deviations at points z_s and rays $\Theta_3(z_s)$ become unequal although the true director is inclined at the same angle Ξ, see figure 1 (b). It is easy to show that, for small D_x and D_y, angles Ψ_1, Ψ_2, and Ψ_3 change from their initial values $\Psi_1 = 0$, $\Psi_2 = 2\pi/3$ and $\Psi_3 = 4\pi/3$ by the magnitudes (2) with $c_1^{(1)} = 0$, $c_2^{(1)} = -\sqrt{3}/\Xi$, $c_3^{(1)} = \sqrt{3}/\Xi$, $c_1^{(2)} = 2/\Xi$ and $c_2^{(2)} = c_3^{(2)} = -1/\Xi$. Figure 1 ($c$) shows a hypothetical situation for the presence of the LPM with a large amplitude that results in a strong (Ising-like) deformation of the unit cell.

The 2-mode unit cell ($m=2$, $k_2 = 1/l$) with the smectic layer coordinates $z_1 = 0$ and $z_2 = l$, in the absence of the long pitch mode, is shown in figure 2 (a). In the presence of displacement $\mathbf{D}$ with projections D_x and D_y along given axes in the 2-mode cell, the director exhibits azimuthal deviations at points z_s shown in figure 2 (b). If $D_x = 0$, the rays $\Theta_2(z_s)$ are equal. If $D_y = 0$ the rays $\Theta_2(z_s)$ are unequal and, in fact, the true director is inclined at different angles Ξ in neighbouring smectic

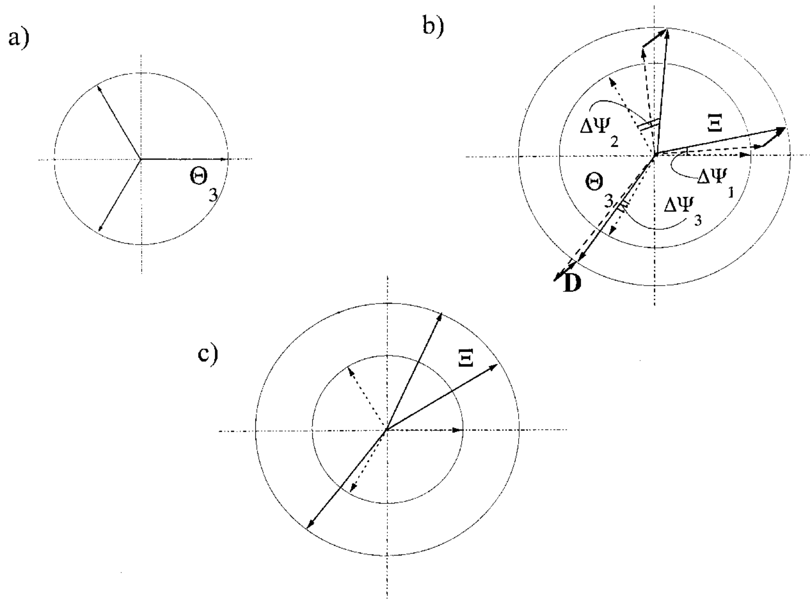

Figure 1. 3 layers-unit cell (3-star) corresponding to a 3-short pitch mode. Arrows show the director projections on the xy-plane in three consequent smectic layers: (a) non-perturbed antiferroelectric 3-star; (b) 3-star in the presence of a weak long pitch mode (a weak ferrielectric, the dotted arrows show the non-equal rays of the antiferroelectric star); (c) 3-star in the presence of a strong long pitch mode (Ising-like ferrielectric).

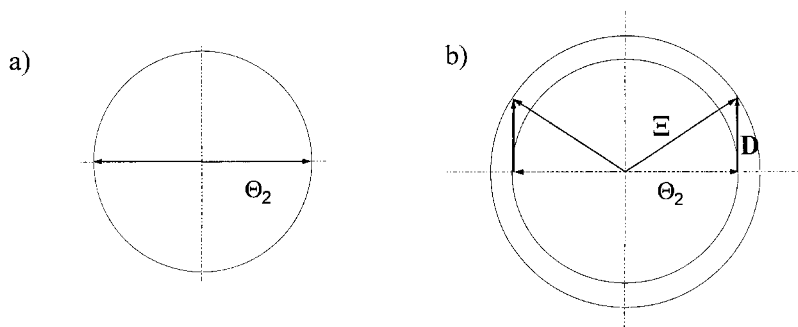

Figure 2. 2 layers-unit cell (2-star) corresponding to a 2-short pitch mode: (a) non-perturbed antiferroelectric 2-star; (b) 2-star in the presence of long pitch mode.

layers, i.e. the layer thickness must make a change that is unprofitable because of a high elastic energy. Therefore, the 2-star should rotate along the z-axis to satisfy condition $D_x = 0$.

3. Free energy densities of non-interacting SPM

The spatially homogeneous part of the free energy density is presented in the form

$$F^* = \sum_j a_j \Theta_j^2 + \ldots \tag{5}$$

where $a_j = a'(T - T_j)$ are the phenomenological parameters, constant a' is positive, temperatures T_j may be different if q_j are not exactly equal to k_j ($j = n$ and $T_j = T_n$ for the n-SPM), $T_j = T_{\mathrm{L}}$ being also different for the long pitch mode with $q_j = q_{\mathrm{L}}$. Since $T_j = T^*$ for $q_n = k_n$, magnitudes T_n are equal to

$$T_n(q_n) \equiv T_n(q_n - k_n) = T^* + C(q_n - k_n)^2 \tag{6}$$

because the transition temperature cannot depend on the sign of incommensurability $\delta q_n = q_n - k_n$. Constant C is positive if the incommensurability is favourable, i.e. if it results in an energy gain.

The spatially heterogeneous part of the free energy density F_q must describe the existence of both the long pitch and short pitch modes Ξ_j. Instead of the magnitude q characterizing the heterogeneous fluctuation terms in the free energy, we choose the more suitable magnitude $X_1 = ql^{-1}/(q^{-2} + v\xi^{-2})$ which helps to describe all the modes, the phenomenological parameter v being determined from the observed line width in X-ray diffraction experiments. In fact, magnitude $\xi/\sqrt{v}$ characterizes the correlation radius in the xy-plane, which can be much more than the correlation radius along the crystalline axis. In the latter case, the short pitch structure is a truly layered structure with a large homogeneous area in the xy-plane. The magnitude X_1 has a maximum value of the order of $\xi/\sqrt{\nu}l$ which is larger than 1. Therefore, it is not correct to develop the free energy as a series in powers of these magnitudes and to set a limit on the powers. It is good practice to think of the free energy as a series in harmonic functions of X_1. In the present simple phenomenological SPM model, just the first harmonics are taken into account. The main non-chiral term is written in the form

$$F_{q,\mathrm{nch}} \propto \sin^2 X_1 = \sin^2\left(\frac{m\pi q l^{-1}}{q^2+\nu\xi^{-2}}\right). \tag{7}$$

Taking into account weak chirality effects, we should include the chiral term depending on the sign of q, for example in the form $\alpha \sin(m\pi/ql)$ at large q, but it should be written as αql at small q, where the small constant α characterizes the chirality. The temperature effects change the intermolecular correlations slightly. The chiral term may be most sensitive to these effects and it may contain the different correlation length $\lambda \cong \xi$. The different $\lambda - \xi$ is dependent on the temperature and vanishes near the SmA–SmC* phase transition point. Thus, the magnitude $X_2 = ql^{-1}/(q^2+\nu\lambda^{-2})$ may also be chosen, and the chiral term is written in the form

$$F_{q,\mathrm{ch}} \propto \beta(\alpha - \sin X_2)^2 = \beta\left[\alpha - \sin\left(\frac{m\pi q l^{-1}}{q^2+\nu\lambda^{-2}}\right)\right]^2 \tag{8}$$

where the parameter α is much less than 1 and the parameter β can be chosen arbitrarily; further $\beta = 1$. Certainly, because of the small difference $\Delta X = X_1 - X_2$ as compared with X, the chiral term can be expanded in powers of ΔX and the first power ΔX-terms describe the harmonics $\cos X$ and $\sin 2X$ with small coefficients. In other words, we are taking into account small corrections to the main term and to the chiral term.

The magnitude $F_q = F_{q,\mathrm{nch}} + F_{q,\mathrm{ch}}$ has a conventional expression for the q-dependent free energy term at small values of q. If the magnitude $q\xi$ is much more than 1, the main term shows that the SPM with $q \cong k$ correspond to minimum energies. The magnitude $(m\xi/2l)$ determines, in fact, a number of possible phases and of transitions between them for a given m-set. The set of chiral smectic phases is described by the minimization of the expression F_q with respect to q. For a given m-set, the n-SPM corresponds to the minimum energy

$$f_n^m(q_n^m) \cong \frac{n^6\pi^2}{m^4}\left[\tau + (-1)^n \frac{m^2\alpha}{n^3\pi}\right]^2 \tag{9}$$

$$\delta q_n^m \cong -\frac{1}{l}\left(\frac{nl^2\nu}{m\xi^2} + (-1)^n \frac{m\alpha}{n^2\pi}\right) \tag{10}$$

where the magnitude

$$\tau = \nu l^2\left(\frac{1}{\lambda^2} - \frac{1}{\xi^2}\right) \tag{11}$$

determines the temperature dependence of the free energy density for each SPM. Each SPM has zero minimum energy at

$$\tau = \tau_n^m = (-1)^{n+1}\frac{m^2\alpha}{n^3\pi}. \tag{12}$$

At the point $\tau = 0$, all the SPM have the same energy

$$f_c = f_n^m(\tau = 0) \cong \alpha^2. \tag{13}$$

The free energy minimum related to a long pitch mode with $q = q_L$ is equal to

$$f_L \cong f_c + 2\left(\frac{\alpha\lambda}{l}\right)^2 \frac{\tau}{\nu} \tag{14}$$

the wave number q_L being equal to

$$q_L \cong \frac{l\alpha\nu}{m\pi\lambda^2}. \tag{15}$$

Thus, the magnitudes f_c and f_L are equal at $\tau = 0$, in the vicinity of this point the magnitudes $f_n^m(\tau)$ being written in the form

$$f_n^m(\tau) \cong f_c + (-1)^n \frac{2\pi n^3\alpha}{m^2}\tau. \tag{16}$$

Comparison of these expressions shows that the slopes of the lines $f_n^m(\tau)$ and $f_L(\tau)$ at the point $\tau = 0$ can either drastically differ or be almost equal in their dependence on the material parameters α and ξ (further, the correlation lengths ξ and λ are measured in molecular lengths l) and on the SPM numbers. Figure 3 shows these features of the SPM behaviour.

The reduced temperature τ describes a change of the chiral term. These effects disappear above the SmA–SmC* phase transition point T_{AC} and they are similar to the observed temperature change in the pitch of the orientational helix. We shall consider τ as a phenomenological parameter. For simplicity, we shall assume that τ is equal to zero at the temperature T_A at which the first phase transition from the smectic A to a chiral smectic with inclined molecules occurs. In general, the inequalities $T_n \neq T_A \neq T_L$ take place, but a difference between these temperatures must be much less than their values, i.e.

$$\tau \propto \frac{T_A - T}{T_A}. \tag{17}$$

Figure 3 throws some light on the observed phase diagrams. In the vicinity of point $\tau = 0$, i.e. in vicinity of temperature T_A, where all the modes have the same

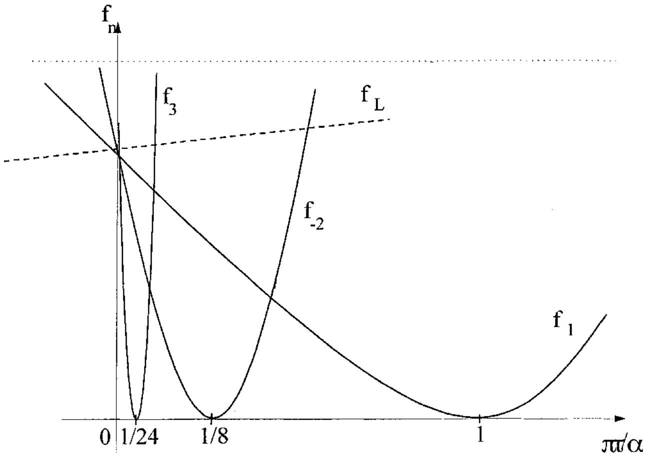

Figure 3. Energy branches of non-interacting SPM as functions of a referred temperature. The heavily dotted curve corresponds to the long pitch mode, the light dotted straight line shows the energy of the homogeneous structure.

energy f_c, a mixing of different modes can actually occur, the long pitch mode being obviously present. It is assumed here that increasing positive values of τ correspond to a decrease of T below T_A. The point $\tau(T_A)=0$ may be slightly below point $\tau(T_{AC})$, i.e. the above mentioned mixing of modes may take place at a temperature which is slightly higher than the temperature of the phase transition to the chiral smectic C phase, T_{AC}. To describe the various phase transitions in detail, we should take into account the interactions between all these modes. This will be done in the following paper. But even the simple approximation of non-interacting modes shows various scenarios of phase transitions between SPM states. For instance, figure 3 shows that the presence of the long pitch mode is essential near the transition point T_{AC}, where some complicated (mixed) orientational states may occur, but, at lower temperatures, the individual SPM (antiferroelectric) states are more probable. It is seen that the SPM with the shortest pitch $2l$ must occur at a lower temperature, and the antiferroelectric state with a larger pitch must appear at a higher temperature. On addition of the long pitch mode to the SPM, ferrielectric states may appear.

It should be noted that the incommensurability $\delta q_n = q_n - k_n$ is present for zero value of chirality parameter α. But, in such a case, the sign of δq_n is not determined, i.e. both the $\pm\delta q_n$ values are equivalent, contrary to the situation with the non-zero α value which determines only the δq_n value and the corresponding minimum energy. Thus, in the case $\alpha=0$, the smectic C film may contain many areas (with size of the order of ξ) which possess weak incommensurabilities of different signs, i.e. on average, the film has no determinate incommensurate structure. In spite of the latter fact, in the absence of macroscopic ferro-, ferri- and antiferro-electric properties, the smectic C film may show a sufficiently strong response to an external field action due to the existence of relatively large correlated areas, i.e. this situation simulates the properties of real polarization-ordered smectic C phases [10]. The latter effects are related to strong possible flexoelectric modulations associated with a highly curved shape of the molecules. These modulations, may have very small pitches, comparable to the smectic monolayer thickness l, and large local polarizations $\mathbf{p}(z_s)$, though the total polarization value in the cell is equal to zero, i.e. the sum $\Sigma_s\, \mathbf{p}(z_s)=0$. Since the smectic planes are isotropic, vectors $\mathbf{p}(z_s)$ can be arbitrarily oriented in the planes, but their absolute values are the same for the z_s-planes. To satisfy the condition $\Sigma_k\, \mathbf{p}(z_s)=0$, vectors $\mathbf{p}(z_s)$ must form the closed manifold geometries shown in figure 4, which coincide with the stars discussed above. The number of such possible geometries is determined by the correlation length ξ since the size of a cell must be less than ξ. For the shortest pitch of the order of l, the $|\mathbf{p}(z_s)|$ value is of the order of d/l^3, where d is an effective molecular dipole moment. On the other hand, $|\mathbf{p}(z_s)| \sim \mu_f/l$, where $\mu_f \sim d/l_2$ is the flexoelectric coefficient. Thus, the spatial modulations with period l may really explain the existence of such antiferroelectric stars.

4. X-ray experiments and SPM approximations

Evidence for the existence of the SPM was recently obtained in experiments on resonant X-ray scattering [11]. This method made it possible to observe directly

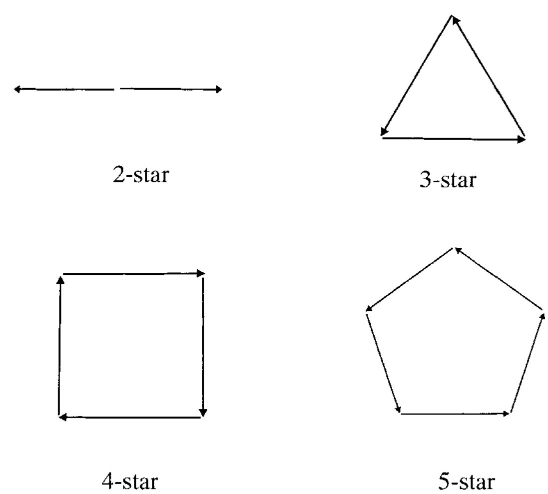

Figure 4. Closed manifold geometries for polarization vectors in the smectic planes, which correspond to various stars in n layers-unit cells, as a result of flexoelectric modulations.

the period of the SPM in ferro-, antiferro- and ferrielectric phases of chiral smectic C LC. It was found that this period is close or equal to an integral number of smetic layers, in particular 2 layers in the antiferroelectric phase, and 3 and 4 layers in ferrielectric phases FI1 and FI2, respectively. Analysis of the heights of the scattering peaks based on the method developed by Dmitrienko [12] shows that the results cannot be explained by structures associated with Ising-like models. At the same time it was concluded that so-called 'clock' structures, which coincide with pure SPMs, can lead to the pictures obtained.

As was shown above, the structure of a real SPM can differ from the ideal 'clock' structure because of the incommensurability of the SPM period with the layer thickness l, and also because of the SPM attenuation by interaction with the long pitch mode. Thus, X-ray scattering on some more complicated structures should be considered.

Steric interactions between neighbouring layers should depend on the angles between their orientations [1]. Thus, if these angles change significantly from layer to layer, as is predicted for example by the Ising-like models, then the molecular density in the N layers-structure should possess more than 1 layer-periodicity (N layers-periodicity if all these angles are different). This should give rise to corresponding convenient non-resonant X-ray scattering peaks. Since they were not observed experimentally, we can conclude that the intermediate angles are almost equal. Therefore we can expect that the attenuation of the SPM is not strong.

To clarify the opportunity for investigation of the subphase structures by means of resonant X-ray scattering, we can assume that the unit cell of the structure contains N smectic layers, the s-th layer of the cell being rotated through the angle Ψ_s relative to the first one. Incommensurability of structure can be considered as the rotation of the t-th cell as a whole about the angle $t\delta$, with respect to some 0-th cell, with $\delta = \pi N l \delta q$. The tensor of susceptibility then can be written as the sum

$$\hat{\chi}(z) = \sum_{t=-\infty}^{\infty} \hat{R}_{t\delta} \hat{\chi}^{\mathrm{uc}}(z + tNl) \hat{R}_{-t\delta} \tag{18}$$

where $\hat{R}_\varphi$ is the matrix of the rotation through the angle φ around the z axis of the SPM, and $\hat{\chi}^{\mathrm{uc}}(z)$ is the susceptibility of a unit cell:

$$\hat{\chi}^{\mathrm{uc}}(z) = \sum_{s=1}^{N} \hat{R}_{\Psi_s} \hat{\chi}^{(0)}(z + sl) \hat{R}_{-\Psi_s} \tag{19}$$

where $\hat{\chi}^{(0)}$ is a single layer susceptibility.

Fourier transformation then yields

$$\hat{\chi}(q) = \sum_{t=-\infty}^{\infty} \sum_{s=1}^{N} \exp[\mathrm{i}ql(tN + s)] \hat{R}_{\Psi_s + t\delta} \hat{\chi}^{(0)}(q) \hat{R}_{-\Psi_s - t\delta}. \tag{20}$$

Since tensor $\hat{\chi}^{(0)}$ is symmetrical, it is convenient to present the production of matrices in the form:

$$\begin{aligned} \hat{R}_\varphi \hat{\chi}^{(0)}(q) \hat{R}_{-\varphi} &= \hat{A}(q) + \hat{B} X_1(q) \exp(\mathrm{i}\varphi) + \hat{B}^* X_1^*(-q) \exp(-\mathrm{i}\varphi) \\ &\quad + \hat{C} X_2(q) \exp(2\mathrm{i}\varphi) + \hat{C}^* X_2^*(-q) \exp(-2\mathrm{i}\varphi) \end{aligned}$$

where

$$\hat{A} = \begin{pmatrix} \frac{1}{2}(\chi_{11}^{(0)} + \chi_{22}^{(0)}) & 0 & 0 \\ 0 & \frac{1}{2}(\chi_{22}^{(0)} + \chi_{11}^{(0)}) & 0 \\ 0 & 0 & \chi_{33}^{(0)} \end{pmatrix},$$

$$\hat{B} = \begin{pmatrix} 0 & 0 & 1 \\ 0 & 0 & i \\ 1 & i & 0 \end{pmatrix}, \quad \hat{C} = \begin{pmatrix} 1 & -i & 0 \\ -i & -1 & 0 \\ 0 & 0 & 0 \end{pmatrix}$$

and $X_1 = 1/2[\chi_{13}^{(0)} - \mathrm{i}\chi_{23}^{(0)}]$, $X_2 = 1/4[\chi_{11}^{(0)} - \chi_{22}^{(0)} + 2\mathrm{i}\chi_{12}^{(0)}]$.

Correspondingly, the susceptibility matrix can be presented as the sum of terms, proportional to $\hat{A}, \hat{B}, \hat{C}$ and their complex conjugate. The term with $\hat{A}$ describes non-resonant scattering with $q = 2\pi t/l$, and the others give resonant scattering on the anisotropic part of the susceptibility. The polarizational properties of the resonant X-ray scattering are determined by the structure of the susceptibility matrix. Following the approach developed in [12], terms with $\hat{B}$ and $\hat{B}^*$ can be associated with type I scattering, which is insensitive to the polarization of the incident wave, while terms proportional to $\hat{C}$ and $\hat{C}^*$ correspond to the type II scattering that does depend on the polarization (see [12] for details).

Then the type I part of equation (20) can be written as

$$\begin{aligned} \hat{\chi}_1 = \hat{B} \frac{1}{N} \sum_{t=-\infty}^{\infty} X_1(Q) \delta\left(Q + \frac{\delta}{2\pi N} - \frac{t}{N}\right) \\ \times \sum_{s=1}^{N} \exp\left[\mathrm{i}\frac{2\pi t - \delta}{N}s + \mathrm{i}\Psi_s\right] \\ + \hat{B}^* \frac{1}{N} \sum_{t=-\infty}^{\infty} X_1^*(-Q) \delta\left(Q - \frac{\delta}{2\pi N} - \frac{t}{N}\right) \\ \times \sum_{s=1}^{N} \exp\left[\mathrm{i}\frac{2\pi t + \delta}{N}s - \mathrm{i}\Psi_s\right] \end{aligned} \tag{21}$$

and the type II part as

$$\hat{\chi}_{\mathrm{II}} = \hat{C}\frac{1}{N}\sum_{t=-\infty}^{\infty} X_2(Q)\delta\left(Q+\frac{\delta}{\pi N}-\frac{t}{N}\right)$$
$$\times \sum_{s=1}^{N} \exp\left[\mathrm{i}\frac{2\pi t-2\delta}{N}s+2\mathrm{i}\Psi_s\right]$$
$$+\hat{C}^*\frac{1}{N}\sum_{t=-\infty}^{\infty} X_2{}^*(-Q)\delta\left(Q-\frac{\delta}{\pi N}-\frac{t}{N}\right)$$
$$\times \sum_{s=1}^{N}\exp\left[\mathrm{i}\frac{2\pi t+2\delta}{N}s-2\mathrm{i}\Psi_s\right] \tag{22}$$

where the dimensionless wave vector $Q=ql/2\pi$ is introduced.

Peaks of the X-ray scattering picture are situated at the positions for which the arguments of δ-functions are equal to zero, and at the same time the other coefficient does not diminish. The latter determines the heights of the peaks that appear to depend on the values of Ψ_s as

$$S^t_M=\left|\sum_{s=1}^{N} \exp\left[\mathrm{i}\frac{2\pi t}{N}s-\mathrm{i}M\Psi_s\right]\right|^2, \quad M=\pm 1, \pm 2. \tag{23}$$

The incommensurability δ is usually small; therefore it affects these coefficients slightly and was omitted above. What is more important, it defines the fine structure of the scattered peaks, since they are split in general into four peaks $Q=t/N-M(\delta/2\pi N)$. Peaks with $M=\pm 1$ are of type I and peaks with $M=\pm 2$ are of type II.

To summarize these speculations we can conclude that as yet the 'clock' structure is not the only one that can explain the pictures of X-ray scattering observed in [11]. In fact, the experimental data obtained can only rule out some concrete sets of Ψ_j, as in the case of Ising-like structures with $N=4$, for which some factors S should diminish or different peaks must have the same height.

Investigation of the fine structure peaks together with polarization measurements can provide some additional information. As a simple illustration of this, we can consider an $N=2$-structure for which splitting of the $Q=K+1/2$ (K is integral) peaks into the doublets $Q=N+1/2+\pm(\delta/4\pi)$ was observed. The structure of the unit cell in this case is determined by only one parameter Ψ_2. It is easy to calculate that

$$S^{2n+1}_{\pm 1}=4\sin^2(\Psi_2/2), \quad S^{2n+1}_{\pm 2}=4\sin^2\Psi_2 \tag{24}$$

which means that observed doublets inevitably define $S^{2n+1}_{\pm 2}=0$ and therefore $\Psi_2=\pi$. We can also predict that these doublets must demonstrate the type I polarization behaviour.

In the case of a pure SPM structure with no attenuation by LPM we have $\Psi_s=2\pi/N(s-1)$. Then the coefficients (23) are non-zero only if $t=KN+M$, which means that peaks are situated at the positions

$$Q=K+\frac{M}{N}-M\frac{\delta}{2\pi N}. \tag{25}$$

Thus, for example, in the $N=3$-phase, double splitting must take place. Particularly, peaks $Q=1/3, 4/3, \ldots$ split into type I peaks with $M=1$ and type II peaks with $M=-2$, while peaks $Q=2/3, 5/3, \ldots$ split into a doublet with $M=-1$ and $M=2$. For the $N=4$-structure, peaks $Q=K\pm 1/4$ do not split at all, being of type I, and peaks $Q=K+1/2$ have double splitting with $M=\pm 2$, being of type II.

Interaction of SPM and LPM perturbs this screw structure of the pure SPM. Comparing equations (10) and (15) it is easy to see that $q_{\mathrm{L}}\ll\delta q$. Thus for our considerations, we can neglect the rotation of the displacement vector **D**, and take into account the SPM incommensurability. To estimate the corresponding changes in the scattering picture, we can study the case of small **D**, when equation (3) is valid. Due to the incommensurability, the unit cell rotates relatively to the displacement, which means that:

$$\varphi_D=-t\delta \tag{26}$$

if the 1st ray in the 0-th cell is oriented along **D**.

The perturbations of Ψ_s give rise to a correction to the susceptibility tensor:

$$\Delta\hat{\chi}(q)=-\mathrm{i}\frac{2D}{\Xi}\sum_{t=-\infty}^{\infty}\sum_{s=1}^{N}\exp[\mathrm{i}ql(tN+s)]$$
$$\times\sin(t\delta+\Psi_s)\frac{\partial}{\partial\Psi_s}[\hat{R}_{\Psi_s+t\delta}\hat{\chi}^{(0)}(q)\hat{R}_{\Psi_s-t\delta}]. \tag{27}$$

Calculations similar to those made above show that this part of the susceptibility also possesses peaks at points (25), but with $M=\pm 1, \pm 2, \pm 3$. Furthermore the polarization type of these peaks differs, so that $M=\pm 2$ peaks are of type I, while $M=\pm 1, \pm 3$ peaks are of type II. Their intensities are relatively small, being proportional to $(D/\Xi)^2$.

Thus, in the case of an $N=3$-structure, interaction of the SPM with a weak LPM slightly changes the polarization features of the scattering picture, but does not give rise to any additional peaks, since $M=\pm 3$ peaks coincide with strong non-resonant ones. In the $N=4$ phase, this interaction also changes the polarization dependence, and, what is more important, it leads to the appearance of new peaks at

$$Q=K+\frac{1}{4}+\frac{3\delta}{8\pi}, \quad \text{and} \quad Q=K+\frac{3}{4}-\frac{3\delta}{8\pi}. \qquad (28)$$

Summarizing our speculations, we can expect that further measurements of peak fine structure, together with experimental determination of polarization features, should give much additional information about details of the structures of sub-phases. It seems that X-ray scattering studies on substances under the action of a constant electric field will also be helpful, especially in the temperature regions of ferrielectrics phases.

5. Conclusions

To describe various families of phase transitions in new liquid-crystalline materials with numerous ferri- and antiferro-electric states, a semi-phenomenological model is proposed which differs from known models in several aspects. There is no conventional series in powers of a small wave number in the heterogeneous part of the free energy density since, in fact, some short pitch waves occur in such liquid crystals and therefore the conventional series is not acceptable. Due to the chiral and polar interactions inside the correlation areas, the real wave numbers q_n and energies of the short pitch packings differ slightly from the basic ones: the wave numbers become incommensurate and change for small magnitudes δq_n which are the measures of the incommensurate structures. To calculate these magnitudes, the following principal approximation, under the present consideration, is made: the free energy is considered as a series in harmonic functions of magnitudes $q/(q^2+v\xi^{-2})$ which well describe the short pitch and long pitch modes. The basic chirality parameter α and the corresponding energy scale α^2 are included in such a series, and the chirality properties are assumed to be dependent on temperature in a conventional manner as linear functions of the temperature close to the phase transition point τ. This model is, in fact, one of the possible approaches; it gives a semi-phenomenological description of the observed variety of polar packings. It seems that the ferrielectric phases appear on addition of the long pitch mode to the SPM or due to the incommensurability of the superlattice in some SPM. In the latter case, the chirality effects, for example in the splitting of X-ray peaks, are even stronger than in the case of the presence of LPM, since the incommensurability δq_n is larger than wave number q_L, see equations (10) and (15). The presence of LPM results in a stronger orientational deformation of the unit cell; for example the cell becomes more Ising-like [see figure 1 (c)], and that could result in additional peculiarities of the molecular density distribution.

The 'family' (2, 3, 4, ...) observed in [11] is one of the possibilities in the framework of our model; it occurs when $m=2$; $n=-2, 3, -4$. The wave numbers of the SPM are equal to

$$q_n \approx \frac{2}{nl}\left[1-\frac{n^2 v}{4}\left(\frac{l}{\xi}\right)^2+\frac{\alpha}{|n|\pi}\right].$$

The first correction in the square brackets is related to the 'superlattice' periodicity in a racemic film, but both the corrections describe the 'optical pitch' periodicity, i.e. the splitting between them is of the order of α/n^2. Thus, this splitting is a maximum for the shortest mode $n=-2$ and may be observed. For larger n, we can predict a lesser splitting of the X-ray peaks and a larger broadening of these peaks, since, in such a case, the incommensurability of the superlattice has the order of $(|n|l^2 v/2\xi^2)$ and increases for larger n. Besides, for larger n the probability of observing a distinct sign of the optical pitch becomes smaller, and the coexistence of both signs of the SPM wave vectors becomes more probable. This also results in a more likely broadening of the scattering peaks.

Financial support from Deutsche Forschungsgemeinschaft is gratefully acknowledged, and S.P. and M.G. are grateful to the Russian Foundation of Fundamental Research (grant 98-02-16802). We thank R. Pindak and V. Dmitrienko for fruitful discussions of experimental results and theoretical aspects.

References

[1] Fukuda, A., Takanishi, Y., Isozaki, T., Ishikawa, K., and Takezoe, H., 1994, *J. mater. Chem.*, **4,** 997.
[2] Takanishi, Y., Hiraoka, K., Agrawal, V., Takezoe, H., Fukuda, A., and Matsushita, M., 1991, *Jpn. J. appl. Phys.*, **30,** 2023.
[3] Isozaki, T., Fujikawa, T., Takezoe, H., Fukuda, A., Hagiwara, T., Suzuki, Y., and Kawamura, I., 1992, *Jpn. J. appl. Phys.*, **31,** 1435.
[4] Hiraoka, K., Takanishi, Y., Sharp, K., Takezoe, H., and Fukuda, A., 1991, *Jpn. J. appl. Phys.*, **30,** L1819.
[5] Orihari, H., and Ishibashi, Y., 1990, *Jpn. J. appl. Phys.*, **29,** L115.
[6] Zeks, B., and Cepic, M., 1993, *Liq. Cryst.*, **14,** 445.
[7] Lorman, V. L., Bulbitch, A. A., and Toledano, P., 1994, *Phys. Rev. E*, **49,** 1367.
[8] Cepic, M., and Zeks, B., 1995, *Mol. Cryst. liq. Cryst.*, **263,** 61.
[9] Pikin, S. A., Hiller, S., and Haase, W., 1995, *Mol. Cryst. liq. Cryst.*, **262,** 425.
[10] Pikin, S. A., 1998, in: Abstracts of the 17th International Liquid Crystal Conference, July 19–24, Strasbourg, France, E1-O2.
[11] Mach, P., Pindak, R., Levelut, A.-M., Barois, P., Nguyen, H. T., Huang, C. C., and Furenlid, L., 1998, *Phys. Rev. Lett.*, **81,** 1015.
[12] Dmitrienko, V. E., 1983, *Acta Cryst. A*, **39,** 29.